



**HAL**  
open science

# Modeling of an Ammonia/Water Absorption Heat Transformer to upgrade low-temperature industrial waste heat both at machine scale and at local scale inside the falling film absorber

Romain Collignon, H el ene Demasles, Hai Trieu Phan

► **To cite this version:**

Romain Collignon, H el ene Demasles, Hai Trieu Phan. Modeling of an Ammonia/Water Absorption Heat Transformer to upgrade low-temperature industrial waste heat both at machine scale and at local scale inside the falling film absorber. *Thermal Science and Engineering Progress*, 2025, 59, pp.103302. 10.1016/j.tsep.2025.103302 . cea-04939332

**HAL Id: cea-04939332**

**<https://cea.hal.science/cea-04939332v1>**

Submitted on 10 Feb 2025

**HAL** is a multi-disciplinary open access archive for the deposit and dissemination of scientific research documents, whether they are published or not. The documents may come from teaching and research institutions in France or abroad, or from public or private research centers.

L'archive ouverte pluridisciplinaire **HAL**, est destin ee au d ep ot et  a la diffusion de documents scientifiques de niveau recherche, publi es ou non,  emanant des  tablissements d'enseignement et de recherche fran ais ou  trangers, des laboratoires publics ou priv es.

# Modeling of an Ammonia/Water Absorption Heat Transformer to upgrade low-temperature industrial waste heat both at machine scale and at local scale inside the falling film absorber

R. Collignon<sup>1\*</sup>, H. Demasles<sup>1</sup> and H.T. Phan<sup>1</sup>

<sup>1</sup>*Université Grenoble Alpes, CEA, Liten, Campus Ines, 73375 Le Bourget du Lac, France*

*\*Corresponding author*

## Abstract

For numerous years, a drastic increase in energy demand has been observed worldwide, mainly originating from fossil fuels, despite an alarming need for a decrease in energy consumption and CO<sub>2</sub> emission. Numerous industries need heat at a high temperature while dissipating heat at moderate to low temperature. Answering this need in an environmentally friendly way is required to mitigate the impact of global warming. In this context, sorption systems are a promising solution able to valorize waste energy at a low electricity cost, up to ten times less electrical power compared to an equivalent vapor compression heat pump. Specifically, Absorption Heat Transformer (AHT) are a type of absorption machine able to recover low-level waste heat ( $\approx 80^\circ\text{C}$ ) in order to provide higher-level heat ( $>100^\circ\text{C}$ ) necessary for vapor production or other industrial uses. In this study, a single stage AHT based on the NH<sub>3</sub>/H<sub>2</sub>O mixture is modeled and simulated. A thermodynamical equilibrium model has been developed to describe the behavior of the machine as a whole. To better describe the absorption process in a grooved vertical plate heat exchanger, a 1D heat exchanger falling film model has also been developed by coupling heat and mass transfer equations between the heat source fluid, the liquid solution and the refrigerant vapor flows. This model allowed to evaluate the minimal size needed to guarantee acceptable performance of the absorber. Results enable to evaluate the performances of the AHT fed by industrial waste heat and cooled by ambient air. The influence of both the waste heat and ambient air temperatures are evaluated. Different coefficients of performance based on the heat transferred and/or the electricity consumption are calculated as well as the expected output temperature of the hot heat sink. The comparison between both model allowed to assess the validity of the simpler equilibrium model to describe the complex absorption process in the case of an AHT and to assess the need of reaching saturation at the absorber inlet, showing that this simple model can be used to precisely describe the performance of an absorber coupling fluid flow, heat and mass transfer. Finally, the range of valuable working conditions for the system are discussed.

## Nomenclature

### Variables

$COP$	Coefficient Of Performance
$GTL$	Gross Temperature Lift [K]
$h$	Enthalpy [J/kg]
$H_w$	Thickness of the wall [m]
$\dot{m}$	Mass flow rate [kg/s]
$L$	Length of the heat exchanger plate [m]
$P$	Pressure [Pa]
$Q$	Heat flux [W]
$T$	Temperature [K]
$W$	Work of a pump [W]
$x$	Mass fraction of ammonia [kg/kg]
$z$	Mass flow fraction of ammonia [kg/kg]

### Greek Letters

$\alpha$	Heat transfer coefficient [W/m <sup>2</sup> ]
$\beta$	Mass transfer coefficient [m/s <sup>-1</sup> ]
$\lambda$	Thermal conductivity [W/m/K]
$\rho$	Volumetric mass density [kg/m <sup>3</sup> ]

### Subscripts

$abs$	Absorber
$adiab$	Adiabatic
$cold$	Cold source
$des$	Desorber
$elec$	Electrical
$evap$	Evaporator
$f$	Fluid
$hs$	Hot source
$i$	Inlet
$int$	Interface
$j$	Component
$o$	Outlet
$sol$	Solution Fluid
$th$	Thermal
$vap$	Vapor
$w$	Wall
$waste$	Waste heat source

## Highlights

- Modeling of an AHT architecture with simple assumptions
- Discrete modeling of coupled heat and mass transfer in a falling film absorber
- Comparison of the AHT architecture model and of the discrete coupled heat and mass transfer falling film absorber model enabled to examine the validity of the assumptions
- Comparison of the simple model with experiments from the literature
- Performances predictions of the system and its capacity to improve waste heat quality

## 1 Introduction

Industrial energy demand represents 32% of the total worldwide energy consumption [1]. This demand has seen a continuous increase over the past decades and is expected to follow a similar trend in the future, despite an alarming need for a decrease in global energy consumption and CO<sub>2</sub> emission [2]. Three-quarters of this industrial energy demand is heat, still largely produced from fossil resources. Ultimately, around half of this heat is rejected into ambient. One of the main limit for recovering the waste heat rejected by industries is their low temperature (<100°C). Thus, few processes can be powered directly from this heat. One solution to valorize this waste energy is to upgrade it to a higher temperature, with thermodynamic machines for example. In the near future, heat pumps will play an increasing role in meeting the industrial demand at a low ecological cost [3]. Specifically, sorption system are a likely solution to valorize waste energy at a low environmental impact compared to conventional vapor compression systems [4, 5, 6]. In this respect, absorption heat transformers (AHT) are able to increase the exergy level of a heat source with minimal mechanical work input, in the form of electricity consumption.

Despite a low exposure, AHT system have known an increasing interest in the industrial sector since the early 1980's, as shown by Cudok et al. [7]. Their review work pointed that high power machines (in the order of 1 MW heating power) are investigated and used to recover waste heat. This work also showed that East Asia have a huge lead in the reported installation of these systems. Today still, most of the reported currently running machines are located in East Asian countries : 12 are in China, 2 in Japan, 1 in Germany, 1 in Italy and 1 in the USA. Most of the reported machines use the H<sub>2</sub>O/LiBr working fluid, which is known for enabling better performances than other working pairs [8]. Heat transformers can also be integrated to district heating network in order to increase their performances and offer a better control of the supplied temperatures as well as future-proofing the installations, as shown by the systems built in Sweden [9] and in Denmark [10].

Quite a number of advanced AHT cycle architectures have been studied in the literature : self driven system without any electricity input [11], double effect cycles that can provide a better Coefficient Of Performance (COP) [12, 13] or multi-stage architecture that enable a higher Gross Temperature Lift (GTL) [14]. Romero et al. [15] evaluated the performance gain of a double-stage heat transformer to an increase in the GTL of 20°C compared to single stage AHT. Comparatively, Hernández-Magallanes et al. [16] reported an increase in maximum GTL of 10°C when using a double-stage system. The modeling work of Donnellan et al. [17] has shown that triple-stage architecture can provide a GTL up to 115°C with a COP around 0.21. Nonetheless, the numerous review works done on the subject of AHT [18, 19, 20] show that for a modest GTL, simple effect single stage system provide the overall best performances.

In the literature, the most investigated working pair is H<sub>2</sub>O/LiBr. This pair has been reported as the overall best performing in terms of heat exchange. However, due to the high corrosiveness and crystallization risk of this mixture, alternative working pairs have been studied. In low temperature applications (< 130°C), the ammonia-water NH<sub>3</sub>/H<sub>2</sub>O working pair enable performances comparable to that of the H<sub>2</sub>O/LiBr and thus can be considered as a better solution for its easier working conditions [18]. Ionic liquids can be added to the mixture [21] to improve the performances of AHT system based on the NH<sub>3</sub>/H<sub>2</sub>O working pair, further reducing the output difference with H<sub>2</sub>O/LiBr. The thorough characterization work done by Garone et al. [22] on a small scale simple effect single stage NH<sub>3</sub>/H<sub>2</sub>O AHT machine showed the potential of the architecture for upgrading low temperature waste heat with a reliable and stable operation.

Despite the growing interest on the subject of AHT development, the range of tools of describing the complete system remain shallow. Most of the reported design processes are based on modeling each component using energy balances based on thermodynamical equilibrium between their input and their output [23]. This method, although valid in almost all cases, is not able to give a precise description of the complex absorption phenomenon occurring in the absorber of the system and are not able to evaluate the temperature levels reached by the solution in the absorber. In the specific case of the AHT configuration, the hot external source entering the absorber is at a higher temperature than any other point of the machine while being expected to heat up thanks to the exothermic absorption reaction occurring within the component. Nevertheless, to the best knowledge of the authors, no reference is tackling the issue of estimating the output temperature of the hot source with a precise description. Some authors assume that the energy generated by the absorption is totally or partially transmitted to the hot source [24], some author assume an arbitrary value for the hot source output temperature based on thermodynamical constraints [17]. Thus, more precise models are needed to

give a better estimation of the capacity of the absorber to elevate the temperature of its hot source, of which a great number of methods have already been developed [25] for a variety of geometry of the heat exchangers. To reduce the size of the absorption machines, compact heat exchanger technologies are often considered. Plate heat exchanger have been proved to offer great performances with relatively small footprints [26]. These heat exchangers have been the object of a great number of studies on their performances in absorber [27, 28, 29] or desorber [30] configurations, evaluating their ideal working conditions and asserting the benefits of choosing this type of heat exchangers.

In this study, the modeling of a small scale  $\text{NH}_3/\text{H}_2\text{O}$  simple effect single stage AHT system is described. This modeling has been designed to size a soon-to-be built 10 kW machine using plate heat exchangers and aiming at upgrading low-grade waste heat ( $60^\circ\text{C}$  to  $90^\circ\text{C}$ ) based on previous knowledge acquired by the group on plate heat exchangers performance [31]. A global model has been developed based on thermodynamical equilibrium, this model is able to give an estimation of the indexes of performance of the machine and to give an estimation of the output temperature of the hot source after flowing through the absorber and has been compared to experimental results. However, the absorber output temperature estimation needs to be further challenged to assess its validity. To help better understand the absorption and heat exchange mechanisms occurring inside of the absorber, a discrete model has also been developed taking account of the coupled heat and mass transfer through the liquid film flow along the plate. The results of both models are compared to evaluate the validity of both descriptions in estimating the performances of the Absorption Heat Transformer. Thanks to the new global AHT model developed, the evaluation of the temperature output of the absorber has been introduced, enabling to quantify the temperature lift provided by the system and further help in quantifying the performance of the AHT architecture.

## 2 System description

The Absorption Heat Transformer (AHT) architecture considered in this paper is represented in Fig. 1. It consists of a simple effect single stage cycle including two internal heat exchangers based on the  $\text{NH}_3/\text{H}_2\text{O}$  pair. The use of a desorber, an absorber, an evaporator and a condenser is usual and necessary in any absorption machine. A separator is placed after the desorber to separate the liquid poor solution from the refrigerant vapor. The two internal heat exchangers are the solution heat exchanger (SHX) and the refrigerant heat exchanger (RHX). These two exchangers are used to recover heat between two sections of their respective line, either the solution or the refrigerant, in order to increase the overall efficiency of the architecture. Two pumps are used to circulate the poor solution and the refrigerant, and an expansion valve allows the rich solution to lower its pressure.

Three heat sources power the machine, a cold source is used at the condenser to condense the refrigerant vapor, a intermediate source (waste heat) is distributed to both the generator and the evaporator to respectively produce the refrigerant and to vaporize the refrigerant. The hot source is flowing through the absorber where it absorbs the heat generated by the exothermic absorption process. Because the waste heat temperature fed to the desorber is quite low ( $< 100^\circ\text{C}$ ), the generated refrigerant vapor is quite pure ( $x \geq 0.97$ ) and there is no need for a rectifier. The waste heat temperature range chosen for this study is  $60^\circ\text{C} \leq T_{waste} \leq 110^\circ\text{C}$  and four different cold source temperatures  $T_{cold}$  will be considered :  $-15^\circ\text{C}$ ,  $0^\circ\text{C}$ ,  $15^\circ\text{C}$  and  $30^\circ\text{C}$ . The external sources fluid is water when the temperature is positive, or a 30/70 mixture of glycol and water and when the temperature

is negative.

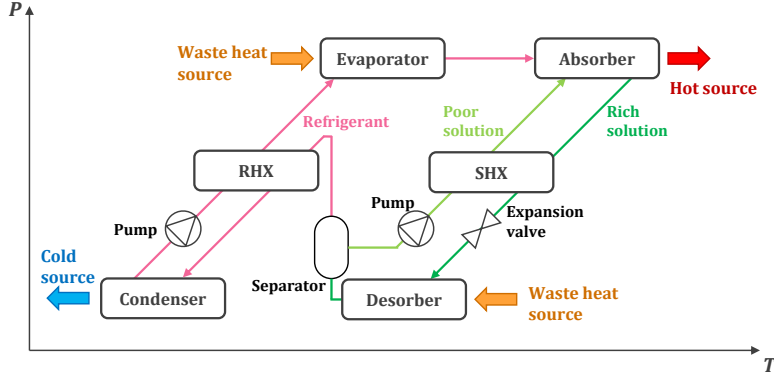


Figure 1 – Scheme of the AHT architecture considered to upgrade the temperature of a low temperature waste heat source.

### 3 Modeling of the AHT and of its absorber

#### 3.1 Global performance model based on steady state equilibrium of the AHT

The behavior and performances of the absorption heat transformer were modeled using steady state thermodynamics equilibrium equations applied to each component of the system. To evaluate the state of the fluid at each point of the machine, energy, mass and species balance equations were applied to each relevant component, considered as open systems. Thus, the mass, species and energy balances applied at each element, each considered as an open system, can be condensed to the following set of equations :

$$Q_j = \sum_f \dot{m}_f h_f \quad (1)$$

$$W_j = \dot{m}_f (h_{f,outlet} - h_{f,inlet}) \quad (2)$$

$$\sum_f \dot{m}_f = 0 \quad (3)$$

$$\sum_f \dot{m}_f x_f = 0 \quad (4)$$

where  $j$  is the considered component, thus, depending on the nature of  $i$ ,  $Q_i$  is the power exchanged at a heat exchanger and  $W_i$  is the work of a pump.  $\dot{m}_f$  is the mass flow rate of the fluid  $f$ ,  $h_f$  is the enthalpy and  $x_f$  is the mass fraction. For the two internal exchangers, the RHX and the SHX, the NTU effectiveness model has been applied with fixed efficiency of 80%. For the other heat exchangers, a temperature pinch of 5°C has been applied. It is assumed that the solution is saturated at the outlet of the desorber, absorber and condenser. The system has been modeled and computed in the equation solver software EES under stationary conditions. This software enables to evaluate the properties of the fluids used in the model. Usually, the Gross Temperature Lift (*GTL*) is one of the quantities used to describe the working conditions of an AHT, which quantifies the increase in heat quality

produced by the AHT. To develop this model, the *GTL* is defined as the difference between the inlet temperatures of the waste heat source  $T_{waste,i}$  and of the hot source  $T_{hs,i}$  :

$$GTL = T_{hs,i} - T_{waste,i} \quad (5)$$

To evaluate the performances of the system, two different Coefficients Of Performance (COP) are calculated. They are the thermal COP eq.(6) and the electrical COP eq.(7), which respectively evaluate the performance of the machine in respect of the absorbed waste heat and in respect of the absorbed electrical power.

$$COP_{th} = \frac{|Q_{abs}|}{|Q_{des}| + |Q_{evap}|} \quad (6)$$

$$COP_{elec} = \frac{|Q_{abs}|}{\sum |W_{pumps}|} \quad (7)$$

This type of model, somewhat conventional, has been thoroughly applied to evaluate the performances of various absorption heat pumps [5, 17, 23] and has proved its validity. However, there is a limit to applying this simple model to an AHT. Despite the possibility to evaluate the performances and exchanged heat power, it is not easy to evaluate the temperature at which the hot source exits the absorber. To evaluate the performances of a single stage AHT system, Jensen et. al. [32] used a similar model but chose to apply fixed pressure levels and temperature elevation in the heat exchangers, as summarized in Table 1. This method allowed to study the performances of the system for a wide range of working conditions, however, this method constrains the absorption process and does not allow for evaluating the spontaneous behavior of an AHT machine in its working environment. To completely characterize an AHT, it is necessary to evaluate both the heat flux transferred to the hot source but also its elevation in temperature. To fully understand what happens at the absorber inlet, we need to look at the thermodynamic state of the solution, and therefore at what happens beforehand. The poor solution leaves the desorber at saturation point, which is at a higher temperature than the absorber inlet due to the absorption process. Then, its pressure is increased by the pump and then is heated in the SHX. After these two stages, the state of the poor solution has been displaced away from saturation. The solution then enters the absorber at a lower temperature than the hot source it is supposed to heat, but as it comes into contact with refrigerant vapor it quickly absorbs a large quantity of ammonia vapor. Because the reaction is exothermic, the solution heats up until it reaches its saturation point. As the energy of reaction is high, the temperature of the solution becomes higher than that of the hot source. To evaluate the increase in temperature of the poor solution, the absorber has been discretized in two section, an adiabatic absorption section and a heat exchange section, as seen in Fig. 2. Between this two sections, the solution is assumed to be saturated. It means that part of the refrigerant vapor has been absorbed by the solution and thus means that the temperature of the

	Sources temperatures	Pressure levels	GTL	Performance indicators
Present model	Input	Input	Input	Output
Jensen et. al.'s model	Input	Output	Output	Output

Table 1 – Table summarizing the whether a parameter in an input or evaluated as an output in the model developed in the present study and the model developed by Jensen et. al. [32].

solution has rose to a value above that of the hot source inlet. The solution is then cooled down by the hot source flow, spreading the distance to its saturated state and thus allowing for more absorption to occur. It is assumed that all of the refrigerant vapor is absorbed at the solution outlet. This assumed behavior allows to evaluate the maximum available temperature inside of the absorber and thus the maximum temperature that can be reached by the hot source at the outlet of the absorber. However, this model is assumed to over-evaluate the maximum available temperature. In a standard plate heat exchanger (as considered in this paper), no adiabatic absorption section can be easily found and thus the solution is exchanging heat with the hot source as soon as it enters the exchanger. To evaluate the validity of this simplified model, a more localized one is needed.

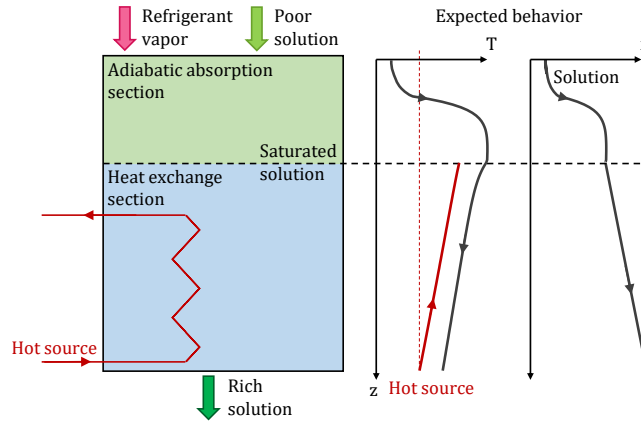


Figure 2 – Scheme of the considered heat and mass transfers behavior for the thermodynamical equilibrium model used to estimate the transfers inside the absorber, where the to-be-heated hot source enters the exchanger at a higher temperature than the solution. In the adiabatic section, the refrigerant vapor is absorbed by the poor solution and reaches the saturated state, as represented at the interface between the two sections. In the heat exchange section, the hot source absorbs heat from the solution. In the process, the solution continues to absorb the refrigerant vapor while its temperature decreases. The assumed temperature  $T$  and solution mass fraction  $x$  behaviors allow for the introduction of a saturated equilibrium point inside of the absorber in order to estimate the maximum temperature reached by the solution.

### 3.2 Validation of the global performance model

To evaluate the validity of the developed model, its results were compared to experiments from the literature. The present model has been compared to experimental results on a simple effect single stage  $\text{NH}_3/\text{H}_2\text{O}$  Absorption Heat Transformer reported by Garone et. al. [22] by evaluating the output of the numerical model obtained from the same source temperatures input as the experiments, the comparison is presented in Fig. 3. Results show a very good agreement between experiment and model on the heat source temperature at the outlet of the absorber  $T_{hs,o}$  with an error under  $\pm 1^\circ\text{C}$ . Regarding the thermal Coefficient Of Performance  $COP_{th}$ , a good agreement is also observed albeit a slight overestimation for the lowest waste heat inlet temperature is obtained. Overall, difference between experiments and model remains under 10% and is even under 5% for most of the cases.

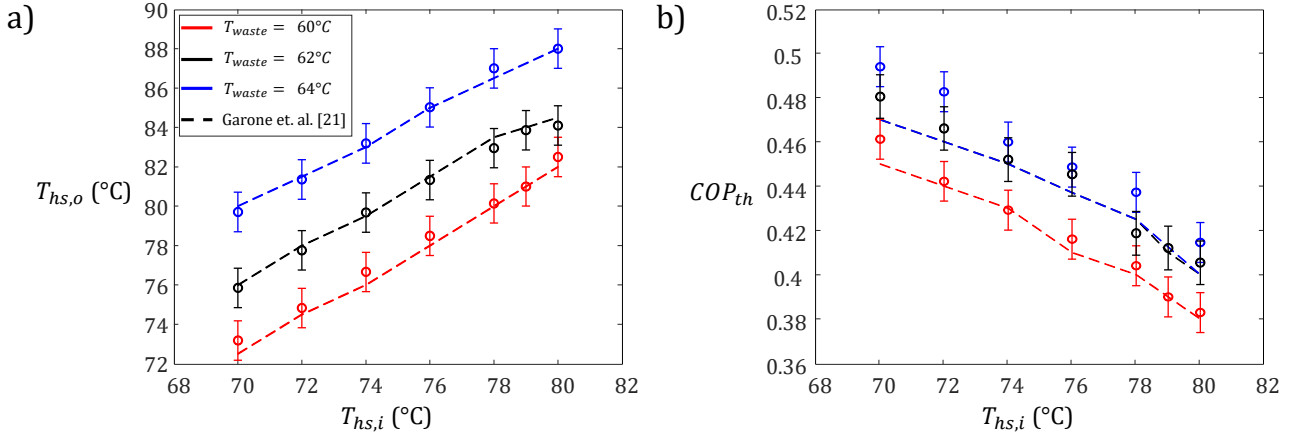


Figure 3 – Comparison of the predicted hot source output temperature (a) and thermal Coefficient Of Performance (b) obtained from the model developed in this paper with the experimental results obtained by Garone et. al. [22]. The inlet conditions of the external sources from the experiments were used as input for the global performance model.

### 3.3 Local heat and mass transfer coupled model of the absorber

To validate the simplified absorber model over a larger working range than the previous experimental data, a comparison with a discretized model is necessary. To this aim, a 1D coupled heat and mass transfer model has been written. This model is an adaptation of the one developed and validated by Wirtz et. al. [31], which was partially rewritten in matlab to allow solving in an AHT absorber configuration. A centered finite difference solving method has been implemented to solve the heat and mass transfer problem, the typical control element considered for solving the problem is schemed in Fig. 4. In this figure,  $\dot{m}$  represents the mass flow rate,  $T$  is the temperature and  $x$  is the species mass fraction, the subscript  $hs$  corresponds to the hot source,  $sol$  to the solution film flow,  $vap$  to the vapor phase,  $int$  to the interface,  $w$  to the wall,  $i$  for inlet and  $o$  for outlet.

The heat exchanger is composed of a vertical wall surrounded on one side by the hot source fluid and on the other side of the solution falling liquid film, on this side is also found the refrigerant vapor. The length of the evaporator is discretized into small element of size  $dz$ . In each of the elements, the energy, mass and species balances of the system are solved under stationary conditions with these assumption :

- The solution film flow is laminar.
- The pressure in the refrigerant phase is considered homogeneous and constant.
- The heat conduction in the wall in the flows direction is negligible.
- The variations of kinetic and potential energies of the fluids are neglected.
- The liquid/vapor interface is at thermodynamical equilibrium.

The different equations as well as the numerical scheme used to solve the problem have been thoroughly described by Wirtz et. al. [31] (eq. (1) to eq. (12) as well as Fig. 2 and Fig. 3) and the model has been validated against experimental data. Thus, a simplified description of the system of equations will be presented thereafter. For each phase, the mass and species balance per unit width equations are :

$$\dot{m}_{sol,i} - d\dot{m}_{NH_3} - d\dot{m}_{H_2O} = \dot{m}_{sol,o} \quad (8)$$

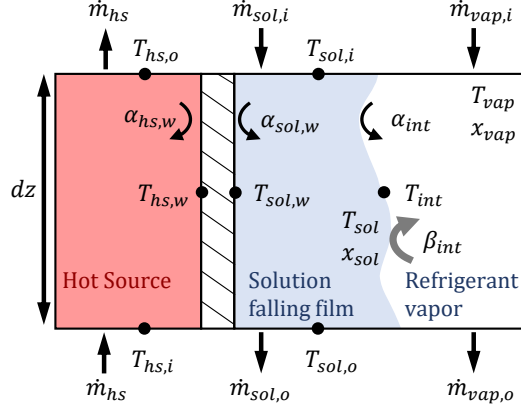


Figure 4 – Diagram of a control element used in the resolution of the coupled heat and mass transfer in the absorber. The hot source (in red) cools down the solution (in blue), resulting in an increase in absorption potential between the solution and the refrigerant vapor. Heat ( $\alpha$ ) and mass ( $\beta$ ) transfer coefficients are used to evaluate the coupled transfer mechanisms in the solution film and at the liquid/vapor interface.

$$\dot{m}_{sol,i} x_{sol,i} - d\dot{m}_{NH_3} = \dot{m}_{sol,o} x_{sol,o} \quad (9)$$

$$\dot{m}_{vap,i} + d\dot{m}_{NH_3} + d\dot{m}_{H_2O} = \dot{m}_{vap,o} \quad (10)$$

$$\dot{m}_{vap,i} x_{vap,i} + d\dot{m}_{NH_3} = \dot{m}_{vap,o} x_{vap,o} \quad (11)$$

where  $d\dot{m}_{NH_3}$  and  $d\dot{m}_{H_2O}$  are the mass flow rates of ammonia and water transferred through the interface during the absorption or desorption process. From these two mass flow rates, the mass flow fraction of ammonia  $z$  transferring through the interface is defined:

$$z = \frac{d\dot{m}_{NH_3}}{d\dot{m}_{NH_3} + d\dot{m}_{H_2O}} \quad (12)$$

It allows to evaluate the thermodynamic equilibrium at the solution film and vapor interface based on the concentration differences between the two phases [33]:

$$d\dot{m}_{NH_3} + d\dot{m}_{H_2O} = \beta_{sol} \rho_{sol} dz \ln \left( \frac{z - x_{sol}}{z - x_{int}} \right) = \beta_{vap} \rho_{vap} dz \ln \left( \frac{z - x_{vap}}{z - x_{int}} \right) \quad (13)$$

As for mass transfer, heat transfer inside of the control element is described thanks to transfer coefficients at each interface. The transfer coefficients used are defined by Goel and Goswami [33] and are denoted  $\alpha$  for heat transfer and  $\beta$  for mass transfer. They are defined as represented in Fig. 4. Thanks to these coefficients, the heat flux between the hot source fluid and the solution falling film  $Q_{wall}$ , between the solution and the liquid/vapor interface  $Q_{sol}$  and between the liquid/vapor interface and the vapor phase  $Q_{vap}$  are defined, per unit width, respectively as:

$$Q_{wall} = dz \alpha_{hs,w} (T_{hs} - T_{hs,w}) = dz \alpha_{sol,w} (T_{sol,w} - T_{sol}) = \frac{\lambda_w}{H_w} dz (T_{hs,w} - T_{sol,w}) \quad (14)$$

$$Q_{sol} = dz \alpha_{int,l} (T_{int} - T_{sol}) \quad (15)$$

$$Q_{wall} = dz \alpha_{int,vap} (T_{int} - T_{vap}) \quad (16)$$

where  $\lambda_w$  is the thermal conductivity of the wall and  $H_w$  is the thickness of the wall. Lastly, the energy balances for the hot source, solution falling film and vapor are defined as:

$$\dot{m}_{hs,i} h_{hs,i} - \dot{m}_{hs,o} h_{hs,o} - Q_{wall} = 0 \quad (17)$$

$$Q_{sol} + Q_{wall} + \dot{m}_{sol,i} h_{sol,i} - \dot{m}_{sol,o} h_{sol,o} - d\dot{m}_{NH_3} h_{sol,NH_3} - d\dot{m}_{H_2O} h_{sol,H_2O} = 0 \quad (18)$$

$$Q_{vap} + \dot{m}_{vap,i} h_{vap,i} - \dot{m}_{vap,o} h_{vap,o} + d\dot{m}_{NH_3} h_{vap,NH_3} + d\dot{m}_{H_2O} h_{vap,H_2O} = 0 \quad (19)$$

The enthalpy  $h$  of the fluid solution, vapor solution and partial enthalpies of the species are calculated through free Gibbs energy equations [34]. In this model, an adiabatic section can be introduced to evaluate the absorption of refrigerant vapor by the solution film close to the inlet of the flow by neutralizing the heat transfer between the hot source and the remaining of the system. It is thus possible to quantify and verify the validity of the assumed behavior of heat and mass transfer through an absorber equipped with an adiabatic section as represented in Fig. 2.

## 4 Results

### 4.1 Global performances of the machine based on thermodynamical equilibrium model

The steady state equilibrium model of the AHT has been used to evaluate the performance of a simple effect single stage Absorption Heat Transformer. The results on the performance indexes are presented in Fig. 5. The evolution of both performance indexes with the cold and waste sources temperatures are presented. In this figure, full lines are the  $COP_{th}$  and dotted lines are the  $COP_{elec}$ . Results show that when the cold source temperature increases, both performance indexes globally decrease. For a chosen cold source temperature, the Fig. 5 show that the AHT system has a finite waste heat temperature working range that becomes narrower as the cold source temperature increases. For example, for  $T_{cold} = 15^\circ\text{C}$ , the AHT is able to provide useful effect only in the waste heat temperature range  $61^\circ\text{C} \leq T_{waste} \leq 98^\circ\text{C}$ . At a fixed  $T_{cold}$ , the performance indexes profiles are slightly shifted with the waste heat source temperature, their respective maximum are separated by 15 to  $20^\circ\text{C}$ . For example, for  $T_{cold} = 15^\circ\text{C}$ ,  $COP_{th}$  is maximum at  $T_{waste} = 93^\circ\text{C}$  while  $COP_{elec}$  is maximum at  $T_{waste} = 78^\circ\text{C}$ . Despite the general decrease in performance with increasing  $T_{cold}$ , the maximal  $COP_{th}$  remains quite high, ranging from 0.7 to 0.6 in the studied region. However, the  $COP_{elec}$  varies much more with  $T_{cold}$ , its local maximal value decrease from 120 to 40 with  $T_{cold}$ . Meaning that the work of the pump is strongly influenced by the working conditions. Nonetheless, in similar working conditions, these performance indexes compare favorably with classical vapor compression heat pump whose only comparable one, the  $COP_{elec}$ , reaches 10 at best [35].

Looking only at the performance indexes is not sufficient to fully characterize the output of an AHT because the useful effect is a result of the absorption process happening inside the absorber, where the hot source enters at an already higher temperature than the solution (as previously described and

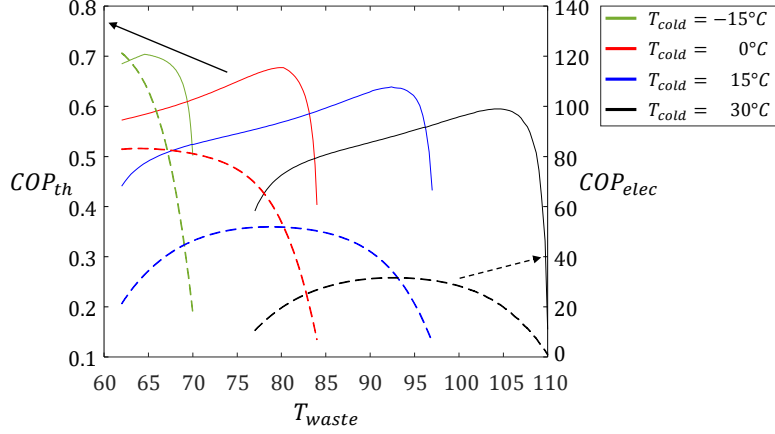


Figure 5 – Estimated performances of the machine depending on the temperature of the cold and waste heat sources. The colors represents different cold source temperatures. Full lines corresponds to  $COP_{th}$  the thermal performance index and the dotted lines corresponds to  $COP_{elec}$  the electrical performance index.

presented in Fig 2). This means that the output temperature of the hot source can not be easily inferred from the solution inlet temperature. To alleviate this unknown, the maximum temperature reached by the solution has been evaluated by assuming a perfect absorption of the refrigerant vapor until the solution reaches saturation and the inlet of the absorber. The estimation of the maximum reachable solution temperature  $T_{sol,max}$  obtained with this method has been represented in Fig. 6 for multiple cold and waste heat source temperatures. As expected, when either the cold source or the waste heat source temperature is increased,  $T_{sol,max}$  increases. The model predicts that for  $T_{cold} = 30^\circ\text{C}$  and  $T_{waste} \geq 100^\circ\text{C}$ ,  $T_{sol,max}$  reaches  $130^\circ\text{C}$  which is the critical temperature of  $\text{NH}_3$  and thus a limit to the operating possibilities of an AHT. It is possible to go beyond this critical temperature because the refrigerant has traces of water vapor mixed with the ammonia, however, the working conditions of the machine changes drastically and a specific architecture is needed to handle the need of supercritical fluids. The couple  $T_{cold} = 30^\circ\text{C}$  and  $T_{waste} \leq 100^\circ\text{C}$  thus looks like a soft limitation for any simple effect single stage  $\text{NH}_3/\text{H}_2\text{O}$  AHT system. Because both  $T_{cold}$  and  $T_{waste}$  influence the response of the system, the better working condition couple in terms of maximum solution temperature is almost never the one where the  $COP_{th}$  is better. As an example, for  $T_{waste} = 95^\circ\text{C}$ ,  $COP_{th}$  is greater when  $T_{cold} = 15^\circ\text{C}$  than when  $T_{cold} = 30^\circ\text{C}$  (as seen in Fig. 5), however,  $T_{sol,max}$  is quite higher in the second case. As a consequence, depending on the need in terms of hot source heating, it is often preferable to design an AHT at a point where the performance is slightly lower but where the recoverable heat is of better quality. Nonetheless, whatever the conditions, the maximum temperature reached by the solution inside the absorber can reach  $T_{waste} + 30^\circ\text{C}$  at best, for this simple effect single stage  $\text{H}_2\text{O}/\text{NH}_3$  AHT architecture. This observation aligns with the results of Jensen et al [32] in similar conditions. The pressures in the machine depends on the cold and waste heat temperature couple values. For the lowest temperatures couples, the pressures in the low and high pressure side are around 2.8 and 8.0 bars absolute. For the highest temperatures, the pressures couple can reach up to 13.5 and 33.5 bars absolute. In the studied range, the pressure levels in the machine thus remain acceptable in order to consider the use of an AHT in real application cases.

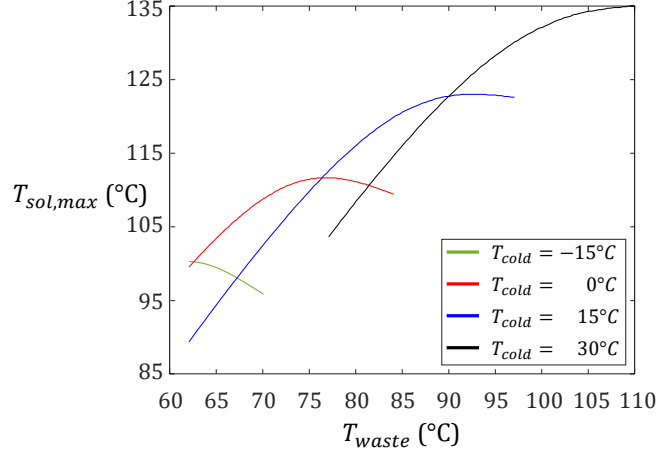


Figure 6 – Evolution of the maximum solution temperature that can be reached inside of the absorber thanks to the absorption process until it reaches saturation depending on the cold and waste heat source temperatures. The colors represents different cold source temperatures.

## 4.2 Evaluation of the performance of the absorber using the local model

To evaluate the performances of the absorber, the local model has been used. The input parameters were obtained thanks to the results of the thermodynamics equilibrium model. The conditions chosen to represent the nominal working point of the AHT is described in Table 2, specifically, it was chosen that  $T_{cold} = 15^{\circ}\text{C}$ ,  $T_{waste} = 80^{\circ}\text{C}$  and  $T_{hs} = 100^{\circ}\text{C}$  and the flow rates were chosen in order to transfer 10 kW of heat to the hot source flow.

	<i>cold</i>	<i>waste</i>	<i>hs</i>	<i>sol</i>	<i>vap</i>
$T$ ( $^{\circ}\text{C}$ )	15	80	100	95	70
$x$ ( $\text{kg}_{\text{NH}_3}/\text{kg}_{\text{H}_2\text{O}}$ )				0.40	0.976
$\dot{m}$ (kg/h)	1300	3000	750	190	35
$P$ (bar)				25.42	25.42

Table 2 – Input properties of the absorber inlet fluids for the discrete model at the nominal working point chosen for the AHT, the flow rates were chosen with the condition of transferring 10 kW to the hot source.

Results from Wirtz et. al. [6, 31] showed that a desorber design consisting of a adiabatic section 10 cm long, a exchange section 32 cm long, 30 cm wide and with 50 plates is sufficient to exchange 10 kW and absorb all the vapor flow in the nominal conditions. This geometry has thus been chosen to study the influence of the adiabatic section length on the heat exchanged to the hot source fluid. Under these nominal conditions and heat exchanger geometry, the evolutions of the temperature the hot source, temperature, mass fraction of ammonia and flow rate of the solution flow as well as the flow rate of the vapor flow are evaluated and represented in Fig 7. Results show a good agreement with the expected evolutions as schemed in Fig 2 under which the AHT global performance model was built. In the adiabatic section, part of the vapor is absorbed until reaching a saturated state where phase change reduce drastically ( $z \simeq -0.05$  m). Upon reaching the heat exchange section, heat is transferred from the solution flow to the hot source flow. The solution flow then becomes slightly

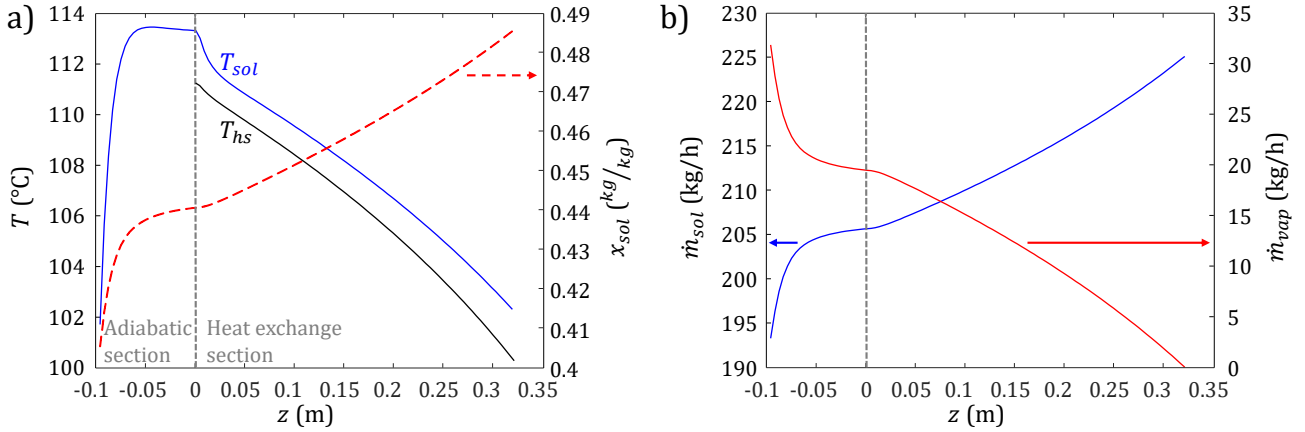


Figure 7 – Evolution of the temperature of the solution film (blue) and of the hot source (black) and of mass fraction of ammonia of the solution film (a) and flow rates of the solution film and vapor flow (b). The solution and vapor are co-currently flowing down the absorber while the hot source is flowing up the absorber, counter-currently to the solution. The studied geometry is obtained from Wirtz et. al. [6], under the nominal working conditions summarized in Table 2.

under-cooled, allowing the absorption process to restart and continue until all of the vapor flow has been absorbed by the solution. With the considered heat exchanger geometry, the totality of the vapor flow can be absorbed by the solution flow, allowing to increase the temperature of the hot source by 11°C between its inlet and outlet of the heat exchange section of the absorber.

For almost half of the adiabatic section ( $-0.05 < z < 0$  m), neither heat nor mass transfer occurs. To improve the complicity of the heat exchanger, a shorter adiabatic section can be considered.

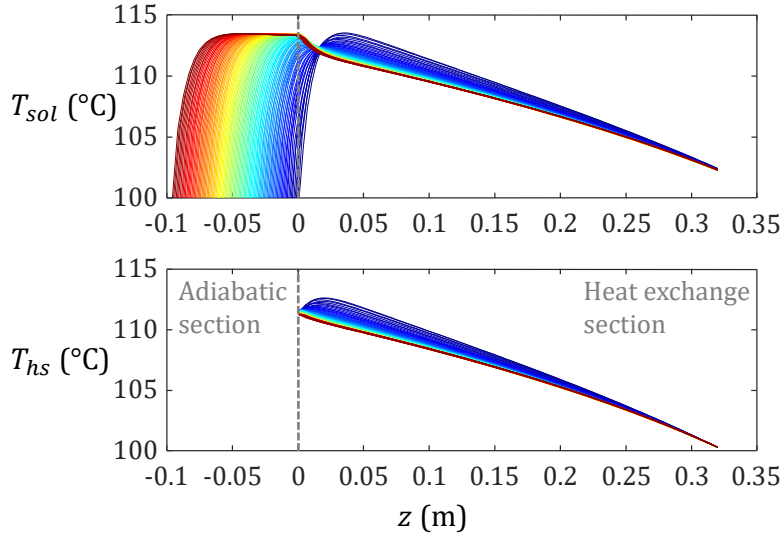


Figure 8 – Influence of the adiabatic section length  $L_{adiab}$  on the bulk temperatures distributions of the solution  $T_{sol}$  and of the hot source fluid  $T_{hs}$  in the absorber in the nominal working conditions. The solution and the hot source fluid are flowing in counter-current configuration. The color of the curves depends on the adiabatic section length, from red for 10 cm to blue for 0 cm. The total heat flux produced by absorption is constant because the flow rates are constant and all the vapor is always absorbed.

Specifically, removing the adiabatic section can be assimilated to using a standers plate heat exchanger as the absorber. The bulk temperature profiles of the solution fluid and of the hot source fluid, are represented on Fig. 8 for adiabatic section length  $L_{adiab}$  ranging from 10 cm to 0 cm. Calculations show that, in the nominal working conditions, an adiabatic length  $L_{adiab}$  of 0.025 m is sufficient for the solution to reach it's saturation temperature before reaching the heat exchange section. It can be observed that under this length, the maximum solution bulk temperature is reached within the heat exchange section (around 0.03 m). In this configuration, the hot source fluid is also reaching its maximum temperature inside of the absorber and is cooled before the outlet. This may seem like a downside but the most important parameter to consider when designing an AHT machine are the heat flux and temperature difference transferred to the hot source fluid. As both the solution and the absorbed vapor flow rate have been maintained constant, the heat flux produced by absorption is also constant. Thus, only the ability of the absorber to transfer energy to the hot source is needed to be evaluated. The temperature difference of the hot source at the inlet and outlet of the absorber  $\Delta T_{hs}$  has been represented as a function of the adiabatic section length  $L_{adiab}$  in Fig. 9. The plot shows that the better configuration in terms of  $\Delta T_{hs}$  is for  $L_{adiab} = 0.015$  m and that increasing its value decrease the temperature difference. Around  $L_{adiab}$  of 0.04 m, the performance drops below the one of an absorber without adiabatic section. Despite an optimal value being found by this model, the temperature difference  $\Delta T_{hs}$  upgrade between no adiabatic section and the optimal length is only of 0.2°C. In the context of building a whole machine, this difference falls within the uncertainties introduced by the different modeling hypothesis. Thus, the introduction of an adiabatic absorption section seems superfluous for its marginal influence.

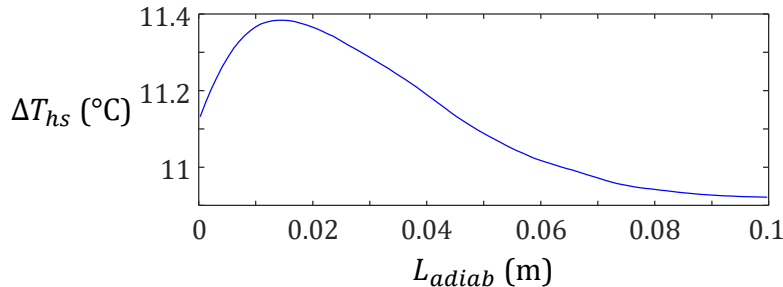


Figure 9 – Influence of the adiabatic section length on the temperature difference between the hot source inlet and outlet from the absorber.

### 4.3 Comparison between the global model and the local model of the absorber output

Because the adiabatic length of the absorber plays very little role on the heat flux transferred to the hot source fluid, considering in the machine equilibrium model that the solution reaches saturation is a reasonable hypothesis to evaluate the behavior of the AHT. To validate the predictions of this model, its results have been compared to that of the discrete model. To this end, the discrete model has been fed all the inlet conditions of the absorber for the total working range studied previously (see Fig. 5 and Fig. 6). The parameter chosen for the comparison is the hot source fluid outlet from the absorber, represented in Fig. 10. The results show a good agreement between both models : except for  $T_{cold} = 0^\circ\text{C}$ , the difference is almost always under 1°C. For  $T_{cold} = 0^\circ\text{C}$ , the deviation is slightly

higher but remains under 2°C. This shown that the simple equilibrium model is relevant when sizing an AHT system and is a good tool in processing relevant experimental data.

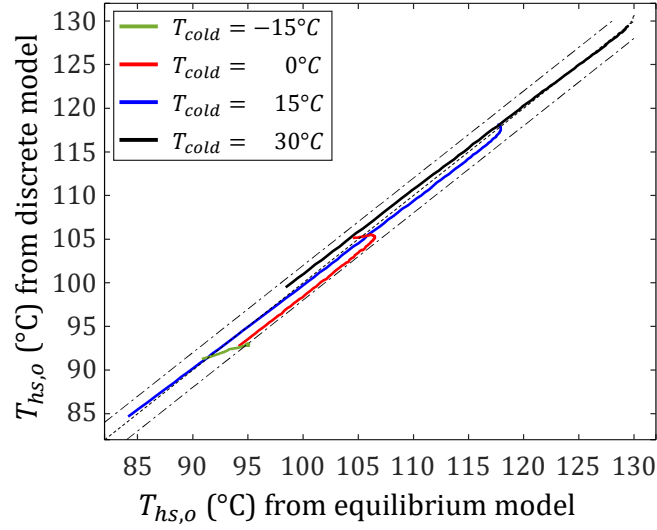


Figure 10 – Comparison of the outlet hot source fluid temperature predicted by both the equilibrium and the discrete model as a function of the cold source and waste heat source temperatures. The colored lines are the results. The dot-dash lines represent the section where the difference between the predictions is less than  $\pm 2^\circ\text{C}$ .

Because both model are in good agreement, the predictions of the equilibrium model are considered relevant to simulate the performance of an AHT. Thus, the ability to heat the hot source fluid estimated by the equilibrium model can be used to define the boundaries of the working range of AHT. The maximum  $\Delta T_{hs}$  that the AHT can produce in the studied working conditions have been presented in Fig. 11. These results show that the maximum temperature difference applied at the hot source fluid is strictly under 12 °C in the studied range. As seen previously, the maximum of  $COP_{th}$  is slightly shifted compared to  $\Delta T_{hs}$ . For example, at the nominal working conditions suggested in Table 2, which is the point where  $\Delta T_{hs}$  is maximal for  $T_{cold} = 15^\circ\text{C}$ , the performance indexes are  $COP_{th} = 0.55$ ,  $COP_{elec} = 49$  and  $\Delta T_{hs} = 10.2^\circ\text{C}$  (see Fig. 5 also). In contrast, the point where  $COP_{th}$  is maximal for  $T_{cold} = 15^\circ\text{C}$ , the performance indexes are  $COP_{th} = 0.62$ ,  $COP_{elec} = 32$  and  $\Delta T_{hs} = 5.5^\circ\text{C}$ . These value show that reaching the best performances only in terms of Coefficients of Performance is not enough to size efficiently an AHT system and that potential hot source flow temperature difference has to be considered.

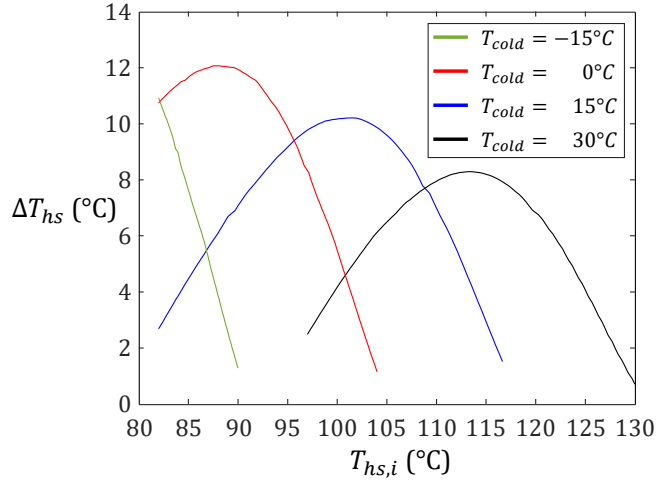


Figure 11 – Maximum temperature difference applied at the hot source fluid  $\Delta T_{hs}$  that can be reached as a function of the hot source fluid inlet  $T_{hs,i}$  for different cold source temperature and a fixed  $GTL = 20^\circ\text{C}$ .

## 5 Conclusion

This study investigates the sizing of a 10 kW  $\text{H}_2\text{O}/\text{NH}_3$  simple effect single stage Absorption Heat Transformer machine used to upgrade heat temperature from an intermediate temperature waste heat source to a hot source. The working range chosen is  $-15^\circ\text{C} \leq T_{cold} \leq 30^\circ\text{C}$  and  $60^\circ\text{C} \leq T_{waste} \leq 110^\circ\text{C}$ . A steady state thermodynamic equilibrium model has been developed to estimate the performance of the system. Classical assumptions are however not sufficient to completely describe the machine, specifically, it is not possible to evaluate the temperature of the hot source output. To evaluate the maximum temperature inside of the absorber, it was assumed that it is composed of an adiabatic absorption section and of a heat exchange section. Between these two sections, the solution is considered saturated. This set of assumption and equations were implemented to estimate the maximum temperature reached by the solution in the absorber and thus the quality of the heat that can be transmitted to the hot source. This model allowed to evaluate the potential as well as the limits of an AHT architecture.

To validate the assumed absorption behavior, a discrete coupled heat and mass transfer absorber model, based on heat, mass and species balance equations was used. This discrete model enable to evaluate the use of the adiabatic absorption section and to validate the assumptions made in the machine equilibrium model. It was shown that the adiabatic section does not play a significant role in the global heat and mass transfer at the absorber as a whole. When describing the component scale behavior of the absorber, the discrete model and the equilibrium model output relatively similar results. Signifying that the assumed behavior of the absorber describes the heat and mass transfer process well enough to be used on its own in the process of sizing the full AHT system.

Finally the models showed that the different performance indexes of the AHT, the output temperature of the hot source, the thermal Coefficient of Performance and the electrical Coefficient of Performance does not attain their maximum for the same sources temperatures. In particular, the conditions where the thermal Coefficient of Performance is high are the conditions where the output temperature of the hot source is quite low. When sizing an AHT, taking account of these shifts is

required. Experimental data on a AHT system based on this architecture would enable further understanding on the transfer processes and allow to refine the assumptions made for the sizing of the system.

## Acknowledgments

The authors acknowledge that this work has been supported by the French Alternative Energies and Atomic Energy Commission (CEA) and the Carnot Energies du Futur Institute.

## References

- [1] IEA. Key world energy statistics, 2021.
- [2] IPCC. Impacts, adaptation and vulnerability - summary for policymakers, 2022.
- [3] IEA. The future of heat pumps, 2020.
- [4] D. Triché, S. Bonnot, M. Perier-Muzet, F. Boudéhenn, H. Demasles, and N. Caney. Modeling and Experimental Study of an Ammonia-water Falling Film Absorber. *Energy Procedia*, 91:857–867, 2016.
- [5] S. Braccio, H.T. Phan, M. Wirtz, N. Tauveron, and N. Le Pierrès. Simulation of an ammonia-water absorption cycle using exchanger effectiveness. *Applied Thermal Engineering*, 213:118712, 2022.
- [6] M. Wirtz, B. Stutz, H.T. Phan, and F. Boudehenn. Performance improvement of NH<sub>3</sub>–H<sub>2</sub>O absorption chiller with a combined generator. *International Journal of Refrigeration*, 144:331–341, 2022.
- [7] F. Cudok, N. Giannetti, J.L.C. Ciganda, J. Aoyama, P. Babu, A. Coronas, T. Fujii, N. Inoue, K. Saito, S. Yamaguchi, and F. Ziegler. Absorption heat transformer - state-of-the-art of industrial applications. *Renewable and Sustainable Energy Reviews*, 141, 2021.
- [8] E. Kurem and I. Horuz. A comparison between ammonia-water and water-lithium bromide solutions in absorption heat transformers. *International Communications in Heat and Mass Transfer*, 28(3):427–438, apr 2001.
- [9] H. Gadd and S. Werner. Achieving low return temperatures from district heating substations. *Applied Energy*, 136:59–67, 2014.
- [10] T. Ommen, W.B. Markussen, and B. Elmegaard. Lowering district heating temperatures – Impact to system performance in current and future Danish energy scenarios. *Energy*, 94(3):273–291, 2016.
- [11] K. Abrahamsson, A. Gidner, and Å. Jernqvist. Design and experimental performance evaluation of an absorption heat transformer with self-circulation. *Heat Recovery Systems and CHP*, 15(3):257–272, 1995.

- [12] Z. Zhao, Y. Ma, and J. Chen. Thermodynamic performance of a new type of double absorption heat transformer. *Applied Thermal Engineering*, 23(18):2407–2414, 2003.
- [13] Yasin Khan, S.M. Naqib-Ul-Islam, Md Walid Faruque, and M. Monjurul Ehsan. Advanced cascaded recompression absorption system equipped with ejector and vapor-injection enhanced vapor compression refrigeration system: Ann based multi-objective optimization. *Thermal Science and Engineering Progress*, 49:102485, 2024.
- [14] Z. Zhao, X. Zhang, and X. Ma. Thermodynamic performance of a double-effect absorption heat-transformer using TFE/E181 as the working fluid. *Applied Energy*, 82(2):107–116, 2005.
- [15] R. J. Romero, S. Silva-Sotelo, and J. Cerezo. First double stage heat transformer (DSHT) in latinamerica. *Chemical Engineering Transactions*, 19(1):149–155, 2010.
- [16] J. A. Hernández-Magallanes, W. Rivera, and A. Coronas. Comparison of single and double stage absorption and resorption heat transformers operating with the ammonia-lithium nitrate mixture. *Applied Thermal Engineering*, 125:53–68, 2017.
- [17] P. Donnellan, E. Byrne, and K. Cronin. Internal energy and exergy recovery in high temperature application absorption heat transformers. *Applied Thermal Engineering*, 56(1-2):1–10, 2013.
- [18] W. Rivera, R. Best, M. J. Cardoso, and R. J. Romero. A review of absorption heat transformers. *Applied Thermal Engineering*, 91:654–670, 2015.
- [19] P. Donnellan, K. Cronin, and E. Byrne. Recycling waste heat energy using vapour absorption heat transformers: A review. *Renewable and Sustainable Energy Reviews*, 42:1290–1304, 2015.
- [20] K. Parham, M. Khamooshi, D.B.K. Tematio, M. Yari, and U. Atikol. Absorption heat transformers - A comprehensive review. *Renewable and Sustainable Energy Reviews*, 34:430–452, 2014.
- [21] I. Sujatha and G. Venkatarathnam. Performance of a vapour absorption heat transformer operating with ionic liquids and ammonia. *Energy*, 141:924–936, 2017.
- [22] S. Garone, T. Toppi, M. Guerra, and M. Motta. A water-ammonia heat transformer to upgrade low-temperature waste heat. *Applied Thermal Engineering*, 127:748–757, 2017.
- [23] A. Sözen. Effect of irreversibilities on performance of an absorption heat transformer used to increase solar pond’s temperature. *Renewable Energy*, 29(4):501–515, 2004.
- [24] W. Rivera, M. J. Cardoso, and R. J. Romero. Single-stage and advanced absorption heat transformers operating with lithium bromide mixtures used to increase solar pond’s temperature. *Solar Energy Materials and Solar Cells*, 70(3):321–333, 2001.
- [25] J.D. Killion and S. Garimella. A critical review of models of coupled heat and mass transfer in falling-film absorption. *International Journal of Refrigeration*, 24(8):755–797, 2001.
- [26] A. Altamirano, B. Stutz, and N. Le Pierrès. Review of small-capacity single-stage continuous absorption systems operating on binary working fluids for cooling: Compact exchanger technologies. *International Journal of Refrigeration*, 114:118–147, 2020.

- [27] J. Cerezo, M. Bourouis, M. Vallès, A. Coronas, and R. Best. Experimental study of an ammonia-water bubble absorber using a plate heat exchanger for absorption refrigeration machines. *Applied Thermal Engineering*, 29(5-6):1005–1011, 2009.
- [28] B. Michel, N. Le Pierrès, and B. Stutz. Performances of grooved plates falling film absorber. *Energy*, 138:103–117, 2017.
- [29] M. Perier-Muzet and B. Stutz. Numerical study of the effectiveness of a vertical falling plate film absorber for an absorption chiller. *International Journal of Refrigeration*, 127:221–229, 2021.
- [30] R. Collignon and B. Stutz. Numerical simulation and modeling of the heat and mass transfer in a grooved flat falling film evaporator. *International Journal of Refrigeration*, 146:148–157, 2023.
- [31] M. Wirtz, B. Stutz, H.T. Phan, and F. Boudehenn. Numerical modeling of falling-film plate generator and rectifier designed for NH<sub>3</sub>—H<sub>2</sub>O absorption machines. *Heat and Mass Transfer*, 58(3):431–446, 2022.
- [32] J. Jensen, T. Ommen, W. Markussen, L. Reinholdt, and B. Elmegaard. Technical and economic working domains of industrial heat pumps: Part 2 - Ammonia-water hybrid absorption-compression heat pumps. *International Journal of Refrigeration*, 55:183–200, 2015.
- [33] N. Goel and D.Y. Goswami. Analysis of a counter-current vapor flow absorber. *International Journal of Heat and Mass Transfer*, 48(7):1283–1292, 2005.
- [34] F. Xu and D.Y. Goswami. Thermodynamic properties of ammonia–water mixtures for power-cycle applications. *Energy*, 24(6):525–536, 1999.
- [35] C. Arpagaus, F. Bless, M. Uhlmann, J. Schiffmann, and S. Bertsch. High temperature heat pumps: Market overview, state of the art, research status, refrigerants, and application potentials. *Energy*, 152:985–1010, 2018.